



# The adsorption of hydrogen on B2 TiFe surfaces

G. Lee<sup>a</sup>, J.S. Kim<sup>a</sup>, Y.M. Koo<sup>a</sup>, S.E. Kulkova<sup>b,\*</sup>

<sup>a</sup>Department of Physics, Pohang University of Science and Technology, Pohang, 790-784, South Korea

<sup>b</sup>Institute of Strength Physics and Material Science of the Russian Academy of Sciences, pr. Akademichesky 2/1, Tomsk, 634021, Russia

## Abstract

We investigate the interaction of hydrogen with the B2 TiFe (001) and (110) surfaces using the full-potential linearized augmented plane wave (FLAPW) method. The changes in the electronic structures in the different B2 TiFe surfaces in comparison with the bulk ground state are analyzed. Ferromagnetic order is found in the Fe-terminated (001) surface with the magnetic moment  $2.27\mu_B$ , which quickly diminishes inside the film. The absorption of hydrogen onto the Fe/TiFe (001) surface results in a decrease in the magnetic moment. For the fully relaxed surfaces interacting with hydrogen, the driving bonding mechanisms for different adsorption sites are discussed. A microscopic explanation of the local surface reactivity is given. It is found that the hydrogen atoms form stronger chemical bonds with the iron atoms than with the titanium atoms in the B2 TiFe surfaces. © 2002 International Association for Hydrogen Energy. Published by Elsevier Science Ltd. All rights reserved.

*Keywords:* Hydrogen storage alloy; TiFe; Hydrogen adsorption; Electronic structure

## 1. Introduction

The electronic structure (ES) of thin films, interfaces, and the two-dimensional magnetism of transition metal (TM) surfaces, is the subject of intense investigation due to increasing interest from both a fundamental and a technological viewpoint. Many surface phenomena are directly related to the electronic structure of the surface. It is well known that the adsorption of atoms on transition metal surfaces can strongly influence their structural, electronic, catalytic and magnetic properties. The surface ES has mainly been investigated for pure transition metals or a monolayer of TM on an inert substrate, while the study of transition metal alloy surfaces using ab initio methods has received less attention [1–7]. One of the most important problems in surface physics is elucidating the mechanism of gas (hydrogen, oxygen, nitrogen, etc.) adsorption onto metal surfaces [8–14]. For example, adsorption of hydrogen or oxygen may

modify the properties of the TM interface growth. Surface oxygen can considerably improve surface order and enhance the magnetic properties of the topmost Fe layers in the TM compounds. Hydrogen can also influence the magnetic properties and phase transformations on the TM surface. Furthermore, the introduction of hydrogen into the V layers in multilayers of Fe and V provides a new approach for the manipulation of interlayer exchange coupling, which can be switched from antiferromagnetic to ferromagnetic [15]. Experiments on TM alloys and their compounds have shown unusual adsorption properties, different from those of the pure metal surfaces [12,13]. Very few theoretical investigations of gas adsorption onto intermetallic alloy surfaces have been carried out [11–15]. To understand this problem at the microscopic level it is first necessary to know the electronic structure of the pure alloy surface. Ab initio calculations of the electronic structure of the surfaces of some intermetallic B2 alloys were recently performed [1–6]. The appearance of surface magnetism in 3d TM alloys was studied in [1,2,4]. The change of ES in the surface layer was considered in more detail [3,5,6]. Thus, the knowledge of the electronic structure of TM alloy surfaces is of particular interest.

\* Corresponding author. Tel.: +7-3822-286848; fax: +7-3822-259576.

E-mail address: kulkova@ispms.tsc.ru (S.E. Kulkova).

Hydrogen plays a crucial role in the properties of various materials. However, the modification of surface electron properties by hydrogen adsorption is not well understood. In contrast to bulk TM alloys and hydrides, the study of their thin films is a relatively new field. TiFe is known to be one of the key materials for the development of a clean hydrogen energy system, and is a well-known intermetallic compound for hydrogen storage [16]. However, TiFe is difficult to activate, but it is believed that the activation of a thin film of TiFe hydride is easy [16]. Despite intensive experimental investigations into the effect of hydrogenation on TM alloy surfaces, the interaction between adsorbed hydrogen and metal is an open question. It should be noted that the electronic structures of bulk TiFe and its hydrides have been investigated in a number of previous studies [17–21]. At room temperature, equiatomic TiFe alloy has a very stable B2-phase in the TiFe-TiCo-TiNi set. This alloy also has composition-dependent magnetic properties, but the origin of its magnetic moment is not clearly understood. It is also known that hydrogen induces the phase transition into a B19 orthorhombic TiFeH structure [22], and TiFe reversibly adsorbs hydrogen [23].

The main goal of the present work is to study the electronic structure of both the clean and hydrogenated TiFe surfaces in order to understand the mechanism of atomic hydrogen adsorption onto the B2 TiFe (001) and (110) surfaces, and to find the microscopic explanation for the local surface reactivity in this alloy.

The paper is organized as follows. In Section 2 we briefly describe the computational details and the full-potential LAPW method used for the electronic structure calculations. Section 3 includes our results for the clean and H-covered TiFe (001) and (110) surfaces, along with a discussion of the results. In Section 4 we summarize the capacity of our model to explain the mechanism of hydrogen adsorption onto TM surfaces.

## 2. Computational details

The FLAPW method (WIEN implementation [24]) within the local density approximation (LDA) for the exchange-correlation potential was applied to band structure calculations of B2-TiFe (001) and (110) surfaces. We have previously parallelized the code for these calculations in the MPI environment for large-scale surface computation [25]. Using the supercell technique, the surface was simulated by repeated slabs separated in the  $z$ -direction by vacuum regions. The calculations were carried out for 5- and 7-layer slabs. A thickness of the vacuum region between the slabs corresponding to three bulk lattice spacings was found to be sufficient to avoid interactions between the Ti or Fe atoms. The experimental lattice spacing  $a = 2.976 \text{ \AA}$  [26] was used in the calculations. The lattice constant for the B2-TiFe alloy obtained from a non-relativistic calculation within the LDA is 0.8% smaller than the measured one. The

lateral lattice parameter was set to the experimental lattice constant for the bulk alloy. The core states were treated in a non-relativistic fashion. The 3s and 3p states were treated as the valence band states. The wave function within muffin-tin (MT) spheres was expanded in spherical-harmonics up to  $l = 10$ . Non-spherical contributions to the charge density and potential within the MT spheres were considered up to  $l_{\max} = 4$ . The electron energy spectrum was calculated at 15 and 72  $k$ -points in the irreducible part of the Brillouin zone (IP BZ) for the (001) surface and at 24  $k$ -points for the (110) surface. Self-consistency was considered to have been achieved when the total energy variation from iteration to iteration did not exceed  $10^{-4}$  Ry. The calculated density of states was broadened by a Gaussian function with a width of 0.2 eV to suppress noise. An electron state is considered as a surface state (SS) if more than 80% of its probability is located in the surface, subsurface planes and the vacuum region.

The simplest surface in B2 transition metal alloys is the (001) surface, which consists of alternating metallic monolayers of Fe or Ti. The idealized TiFe (001) surface can be terminated by either Ti or Fe atoms, although there is no experimental data on the relative stabilities of these two surface terminations. In the present paper both Ti- and Fe-termination of the B2 TiFe (001) surface are considered; these variants are denoted by Ti/TiFe and Fe/TiFe, respectively. Another surface in B2 TiFe is the (110) surface. In this case each layer is a rectangular lattice consisting of Ti and Fe atoms with the same stoichiometry as the bulk ground state. The interlayer distances were optimized with a damped Newton dynamics for free films consisting of 5 substrate layers for TiFe (110), and 7 substrate layers for TiFe (001). The forces at the atoms were calculated according to [27]. Initially, the adsorbate was placed at a distance roughly equal to the value of the metal-hydrogen bond distance. This choice did not need to be especially accurate because the hydrogen layer and substrate layers were allowed to relax. A number of different adsorbate sites were considered for the (110) surface, while hydrogen was placed only in the hollow site for the (001) surface. We assume a  $p(1 \times 1)$  coverage of H on the TiFe surface.

## 3. Results and discussion

### 3.1. The clean TiFe (001) and (110) surfaces

As the first step in our calculations we calculated the electronic structure of the clean TiFe (001) and (110) surfaces. Fig. 1 shows the calculated local density of states (LDOS) for the 7-layer Ti/TiFe (001) and Fe/TiFe (001) films. All data given in this section refer to unrelaxed surfaces. Comparison of the LDOS for the central and the first-from-center layer in the (001) surface with the electronic structure of the bulk B2-TiFe alloy (the dotted curves in Fig. 1) shows

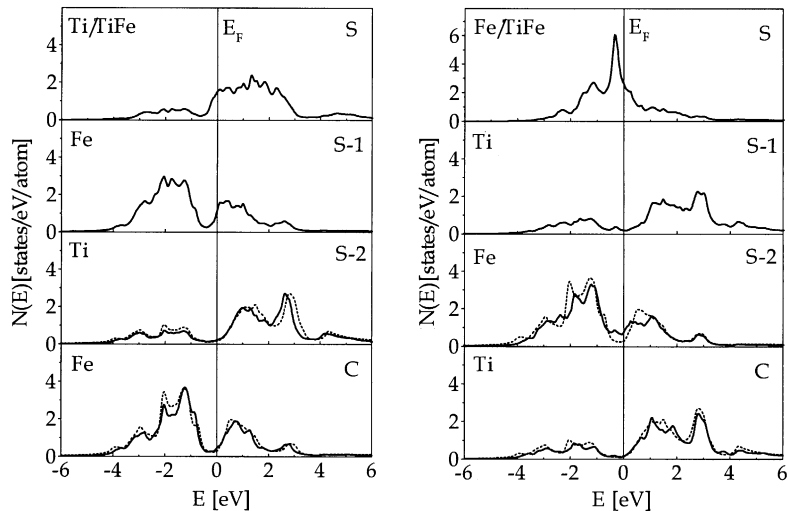


Fig. 1. Local density of states for 7-layer Ti- and Fe-terminated TiFe (001) films (solid lines). The symbols C, S-2, S-1 and S denote the central, first from central, subsurface and surface layers, respectively. Bulk LDOS are plotted with dashed lines. The calculated LDOS was broadened by a Gaussian with a width of 0.2 eV.

that the bulk region is accurately represented in the surface calculations. In addition, the properties of the central layer for the 5-layer TiFe (110) were found to coincide well with those of the bulk alloy. A significant change in the surface LDOS compared to that for the S-2 layer is observed for both surface terminations; however, the effect of the surface is already much weaker in the subsurface layer. The change in ES is related to charge redistribution near the surface and the appearance of the surface states. The charge decrease in the surface layer is due to the reduction in the number of nearest neighbors at the surface (in the bulk each atom has 8 nearest neighbors, whereas on the (001) surface an atom has only 4). The ES changes are more significant for the Fe/TiFe (001) surface, and result in a sharp peak at around  $-0.3$  eV (Fig. 1b). In the Fe/TiFe (001) case the changes rapidly diminish with the depth into the film, whereas for Ti/TiFe (001) they are less significant but more pronounced inside the film. Note that LDOS obtained for both termination of the B2 TiFe (001) surface are in good agreement with the results of tight-binding calculations of this surface reported recently by Canto et al. [5]. On both surfaces there are many so-called Tamm surface states, which are pulled out of the bulk d-bands continua and stem from perturbations of the crystal potential at the surface (by bulk/surface potential shift). There are also the Shockley SS, states that resemble “dangling bonds”, which are located in the bulk band gaps. All of the surface states are basically d-type, with only a few states containing significant portions of s- and p-symmetry. More details are found in [6]. In general, the surface states observed in the pure metals are also present in the surface of the TM alloy.

If the surface of the material consists of ferromagnetic atoms, there is a magnetic moment at the surface even though

it is absent from the bulk state. Since iron is known to be a good magnetic metal, we also investigated the possibility that a ferromagnetic surface layer be formed in the Fe/TiFe (001) film. To achieve this we performed spin-polarized calculations within the LSDA. The local spin densities of states for the Fe/TiFe (001) film are shown in Fig. 2. In general, the results show similar trends to those observed for the non-magnetic case. As seen from Fig. 2, the LDOS structure of the central layers differs insignificantly for the majority and minority spin, and it is very similar to that obtained in the paramagnetic calculation (Fig. 1). In addition, d-resonance states are observed in the surface layer of Fe/TiFe (001). The maximum of the LDOS lies at the Fermi level for the minority spin, whereas for the majority spin it is at  $-2.0$  eV. The exchange splitting of states with opposite spin, combined with the narrowing of the d-bands, results in the appearance of the magnetic moment at the surface, which is equal to  $2.27\mu_B$ . Hence, the surface layer exhibits an enhanced magnetic moment compared to the Fe bulk value ( $2.22\mu_B$ ), although this value quickly decreases inside the film, having diminished to  $0.41\mu_B$  by the first-from-central layer. This effect may be a result of a finite slab thickness. Our results also reveal that Fe induces a small polarization in the subsurface layer, and the magnetic moment of Ti is negative ( $-0.41\mu_B$ ), which is in good agreement with the result of [1,2]. A similar result has been reported recently for the B2 FeV (001) surface [28]. The Ti-terminated (001) surface is non-magnetic. Calculation of the total energy shows that ferromagnetic ordering on the Fe/TiFe (001) surface is energetically favorable, with a 0.87 eV lower total energy. Unfortunately, we did not consider the possibility of different magnetic ordering (in particular antiferromagnetic ordering) in the present work as was done for FeV in [28]

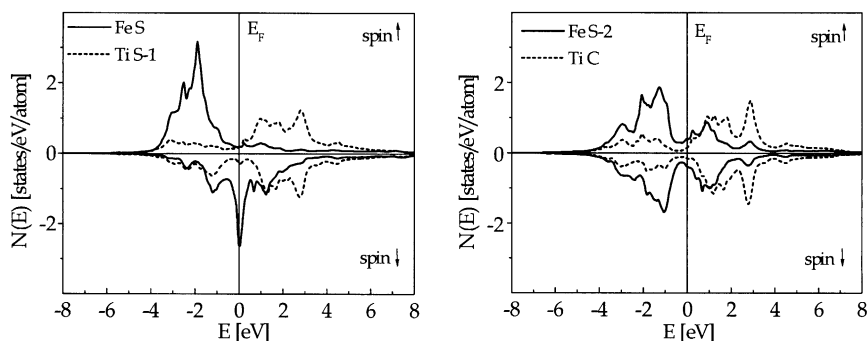


Fig. 2. LDOS of the different layers for the magnetic Fe/TiFe (001) system. Fe bands are plotted with solid lines and Ti bands with dashed lines.

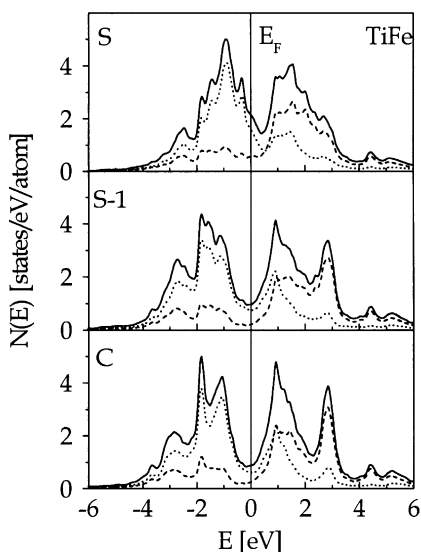


Fig. 3. Total and local DOS for 5-layer TiFe (110) film: total DOS is given by solid line, local DOS of Fe and Ti are given by dotted and dashed lines, respectively.

because this takes too much computational time with the FLAPW method.

The (110) surface of B2 TM compounds has received greater attention in the past studies, which mostly examined NiAl [11–13,29,30]. In Fig. 3 we present the total and local DOS for a 5-layer TiFe (110) film. The decrease in charge observed in the surface layer of this system is mostly due to s- and p-electrons ( $\sim 10^{-2}$  electrons (el.)), whereas the change in charge due to d-electrons is an order of magnitude less ( $\sim 10^{-3}$  el.). Analysis of different charge contributions ( $dt_{2g}$  and  $dc_g$ ) indicates covalent binding at the (110) surface. It decreases insignificantly in comparison with bulk, which is ascribed to the presence of different atoms in the layer, and to the smaller distance between atoms within one layer. We would like to emphasize that surface effects are

confined mainly to the surface layer in the case of the (110) surface, and do not spread into the solid (top panel in Fig. 3). This is consistent with the short screening length in transition metals. The influence of the surface decreases faster in the (110) film because its interlayer spacing is greater than that of the TiFe (001) film ( $d_{110} = \sqrt{2}d_{001}$ ). In general, the surface ES has similar features to those in the bulk. Basically a redistribution of states into d-subbands is happening. Moreover, there is no strong splitting into subbands connected to  $t_{2g}$  and  $e_g$ -symmetry in the surface layer, as is found in the bulk. The density of states at the Fermi level ( $N(E_F) = 2.27$  el./eV/cell) increases in comparison with the bulk (0.39 el./eV/cell). It is known that the relatively high chemical activity of the transition metals and their alloys is caused by a high DOS at the Fermi level ( $E_F$ ). Thus, the present results indicate that the clean TiFe (110) surface and the TiFe (001) surface cannot be inert. Calculations of X-ray absorption spectra and electron energy-loss spectra [6] showed an increase in absorption on the different surfaces in comparison with the bulk.

### 3.2. Hydrogen adsorption onto TiFe (001)

The adsorption of atomic hydrogen was investigated for both terminations of the TiFe (001) surface. Starting with a non-magnetic seven-layer film, we relaxed the layers and found a contraction of the interlayer distance between the surface and subsurface layer of  $-25.6\%$  for Fe/TiFe and  $-13.9\%$  for Ti/TiFe, whereas the second interlayer distance expanded by  $1.5\%$  in both cases. These values did not change significantly when the two innermost layers were fixed at the bulk coordinates. Unfortunately, structural characterization data of the TiFe (001) surface is not available. Similar behavior was recently reported for the non-magnetic Fe (001) film [31], which showed an inward relaxation of  $-20.7\%$  within the general gradient approximation (GGA) [32] for the exchange-correlation potential. The relaxation for the Ti-terminated surface can be compared with the result obtained by Bihlmayer et al. for V (001) [31], which

showed a  $-11.1\%$  relaxation of the first interlayer distance. A recent calculation of  $V(001)$  within the framework of the projector-augmented wave (PAW) method [33] displayed an even stronger inward relaxation of  $-13.6\%$  for the first interlayer distance, and a small outward relaxation of  $1.0\%$  for the second spacing. Bihlmayer et al. [31] showed that the relaxations change very little on going to a 15-layer  $V(001)$  film.

There are several possible high-symmetry positions for the adsorbate on the TiFe (001) surface. In the present work we do not consider the top and bridge positions because the hollow position is known to be the most stable adsorbate site in transition metals [10]. The preference for the fourfold hollow position on the (001) TM alloy surface for hydrogen adsorption is related to the higher coordination number at this site, and to the minimization of the repulsion between the overlapping charge densities of H atoms as well as the surface and subsurface TM atoms. The hybridization of the metal d-states with the s-orbital of the adsorbate can be used for selection of the most stable adsorbate site, because  $N(E_F)$  alone is insufficient to differentiate between the TM surfaces [10,34]. In addition to a relaxation of the clean surface we found a minimum of the adsorption energy, which was calculated as a function of the distance between the H atom and the surface layer. The quasi-static movement of hydrogen perpendicular to the surface will not represent the real situation because temperature effects are not taken into account. Moreover, the substrate and adsorbate geometries need to be relaxed to lower the energy of the final equilibrium position. Unfortunately, relaxation of the adsorbate/substrate complex remains a formidable computational task.

The minimum in the adsorption energy ( $E_{ad}$ ) is observed at practically the same H position as in pure Fe [8] (around the distance of the Fe–H bond length  $\sim 1.8 \text{ \AA}$ ). The values obtained were  $1.74 \text{ \AA}$  for Ti/TiFe and  $1.88 \text{ \AA}$  for Fe/TiFe, which represent the distances between the adsorbed H atom and the Fe or Ti subsurface atoms. The calculated binding energies ( $E_b$ ) are  $-3.12$  ( $-3.15$ ) and  $-3.09$  ( $-3.3$ ) eV and the corresponding adsorption energies are  $-0.75$  ( $-0.78$ ) and  $-0.73$  ( $-0.97$ ) eV for Ti/TiFe and Fe/TiFe (001), respectively. The values in parentheses are the adsorption and binding energies for the unrelaxed surfaces. The energies  $E_b$  and  $E_{ad}$  were calculated in accordance with the equations given by Eichler et al. [10]. The binding energy is defined as the difference between the total energies of the hydrogen-covered and clean surfaces plus the total energy of the appropriate number of free hydrogen atoms. The adsorption energy is defined as the energy difference between the hydrogen-covered and clean surfaces plus the total energy of the hydrogen molecules. The values of  $E_b$  and  $E_{ad}$  are given with respect to the number of the hydrogen atoms. We used experimental values of  $E_H = -13.6058 \text{ eV}$  for the total energy of the H atom and  $-4.75 \text{ eV}$  for the binding energy of the  $H_2$  molecule [35]. The calculated value  $E_H = -12.6861 \text{ eV}$  (LDA) is less than the experimental

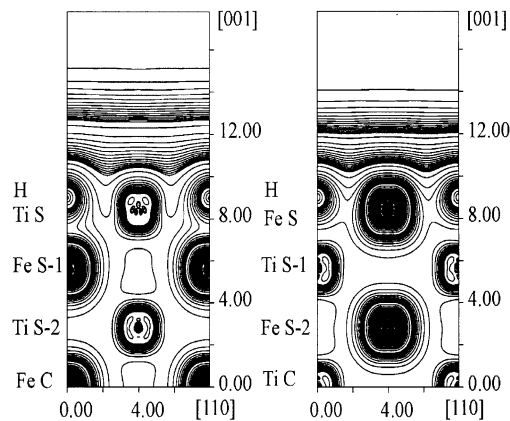


Fig. 4. A contours plot of the charge-density distribution in a [110] plane perpendicular to the (001) surface for H/TiFe (001) with H atoms adsorbed in the fourfold “hollow” position.

value. The adsorption energy depends on the approximation used for the exchange-correlation potential, and the values of  $E_b$  presented here, calculated within LDA approximation, seem to be slightly overestimated. It is known that the binding energy of hydrogen in 3d TM is around 3 eV, and a small variation in  $E_b$  is found across the 3d TM series [36]. The value of  $E_b$  for Ti is slightly lower than that for Fe [36].

Fig. 4 shows a contour plot of the charge density distribution in the plane perpendicular to the (001) surface and extending along the [110] direction for each surface termination, with the hydrogen in the fourfold hollow position. Since the hydrogen is located deep within the TiFe (001) surface, a definite smoothing of the charge-density corrugation is obtained in the vacuum region. As seen from Fig. 4, a region of relatively high electron density is observed from the H site to the Fe site. Despite the greater affinity of Ti atoms for hydrogen in comparison to Fe atoms in binary metal–hydrogen systems, the present results show that the hydrogen has a greater affinity for Fe atoms than for Ti atoms in the cases considered. This occurs despite the fact that the Ti atoms are the nearest neighbors of H in the Fe/TiFe (001) system. A similar result was obtained by Yukawa et al. for TiFe [37] in calculations using the cluster approach. These authors also showed that the magnitude of Me–H bond order increases when an alloying metal with a large charge is added to TiFe. It is well known that TiFe forms two hydrides in the bulk state:  $FeTiH_x$  with  $x = 1.0$  and  $2.0$  [22]. Changes in the chemical bonds between the Ti, Fe and H atoms determine the relative stabilities of the TiFe hydrides.

Fig. 5 gives the LDOS for the surface and subsurface atoms for both TiFe (001) surface terminations with hydrogen in the hollow position. The hydrogen 1 s-states are located at around 5 eV below the Fermi level ( $E_F = 0$  in Fig. 5) for the Fe-terminated surface, and they lie deeper at  $-6.3 \text{ eV}$

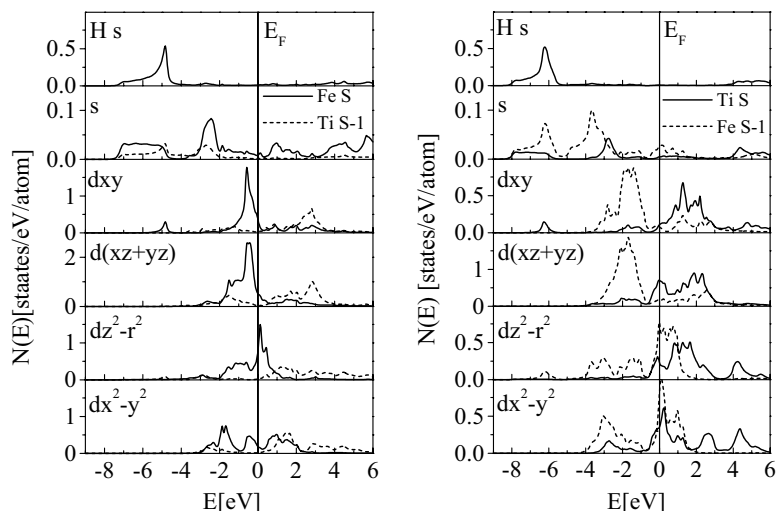


Fig. 5. Partial DOS in the surface (solid lines) and subsurface (dashed lines) layers of the substrate and on the adsorbate H site for H/TiFe (001) with H atom in the “hollow” position.

for the Ti-terminated case. The hybridization of these states with the d bands of Fe and Ti is localized in real space, and only the surface and subsurface metal atoms have peaks at the same energies. The interaction of hydrogen with surface Fe atoms in Fe/TiFe, and with subsurface Fe atoms in Ti/TiFe, is much stronger than the corresponding interaction with Ti atoms for both surface terminations. Moreover, the binding in the fourfold hollow position occurs in Fe/TiFe through the formation of bonding H s–Fe  $d_{xy}$ -states, whereas in Ti/TiFe the hydrogen interacts with both the subsurface Fe  $d_{z^2-r^2}$  states and the surface Ti  $d_{xy}$ -states. However, in both cases the bonding states are formed at relatively high binding energies. In the present calculations, the central layers of the film do not contain hydrogen and show a very small DOS below  $-4$  eV. Hydrogen could influence the states of the central layers only indirectly, through hybridization with neighboring atoms. In general, however, hydrogen introduces only a minor change in the surface electronic structure. Due to an increase in the number of the valence electrons caused by hydrogen charging, the Fermi level shifts to the region with a high density of states. The increase in  $N(E_F)$  for the H-covered Ti-terminated surface also indicates the possibility of the reconstruction of the surface. Hence, the partial DOS are very useful for understanding the local chemical reactivity of the TM alloy surfaces and this specific interaction between the hydrogen atom and the surface of material is one of the determining factors in kinetics of a solid–gas reaction.

For the ferromagnetic Fe-terminated TiFe (001) surface, the addition of hydrogen results in a decrease in the magnetic moment of the Fe atoms ( $1.81\mu_B$ ). The adsorption energy is  $-0.72$  eV for unrelaxed surface. On the other hand, the adsorption energy for the Ti-terminated film shows no

significant change because the Ti-terminated film is nonmagnetic. It is believed that these values change insignificantly if the relaxation is taken into account. The magnetic moment of the Fe subsurface atoms is  $0.83\mu_B$  for the H-covered Ti-terminated film, but is only  $0.29\mu_B$  for the clean surface. It is not obvious that in the H-covered Ti-terminated film this is an effect of the finite size of the film. For detailed investigation of the oscillation of the magnetic moment in the plane perpendicular to the surface it is desirable to consider much thicker film. The induced polarization of the surface Ti atoms increases slightly on adsorption of H from  $0.15$  to  $0.23\mu_B$ . The present results are very similar to those obtained by Ostanin et al. for V/Fe superlattices [15]. In addition, it should be noted that the hydrogen adsorption perturbs the metal d-orbital occupancies, especially those involved in the metal–hydrogen bonding. The number of bonding states decreases slightly for the H-covered Fe-terminated surface because of the transfer of d-electrons into antibonding levels above the Fermi level. For the subsurface Fe atoms, however, the occupancies of the d-bonding levels are found to be increased. In the present work we do not investigate the alteration of the surface electronic structure as a function of the hydrogen concentration; these results will be presented in the future. In general, the results obtained for the non-magnetic and magnetic cases clearly indicate that the Ti-terminated surface is slightly preferable for hydrogen adsorption on the B2 TiFe (001) surface.

### 3.3. Metal–hydrogen on the (110) surface

The (110) surface has four different high-symmetry adsorption sites: on top of a substrate atom (Fe-T and Ti-T in Fig. 6), and in a position that forms a bridge between two

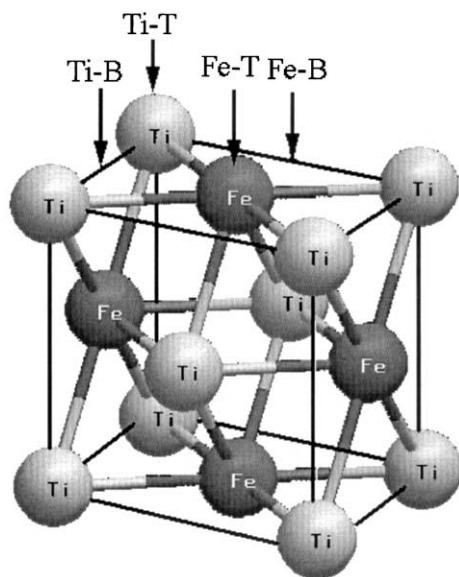


Fig. 6. The calculated H adsorption sites on the TiFe (110) surface. Ti-T and Fe-T denote H adsorbed on-top of Ti or of Fe atoms and Ti-B and Fe-B mark H adsorbed on a bridged site between Ti or Fe atoms.

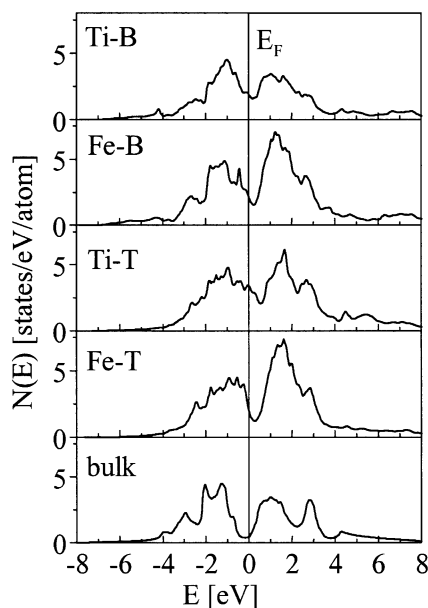


Fig. 7. The evolution of the surface DOS in H-covered TiFe (110) films for each H site.

nearest-neighbor surface atoms (the Fe-B and Ti-B positions). Fig. 7 shows the total surface DOS for the H-covered TiFe (110) film for each H adsorption site. The distances between the adsorbed H atom and the Fe or Ti subsurface

atoms are 1.8 Å for the top position and 1.14 Å for the bridge position. Conclusions about the relative stability of phases are often derived from comparison of their  $N(E_F)$  values. When no hydrogen is adsorbed, the DOS at the Fermi level is significantly lower than the DOS obtained in any of the cases with adsorbed hydrogen (Fig. 7). Of the four adsorption sites considered, the most unstable geometry is the Ti-top position. In this case the Fermi level lies exactly on the peak in the DOS. This peak is located between the two main sharp peaks, which are due to the Fe and Ti atoms. As seen in Fig. 8, which gives the partial DOS of the H, Ti and Fe surface atoms, this peak at the Fermi level is formed mainly by contributions from H and Ti. Adsorption of H at the Ti-T position allows for the formation of the chemical bonding of the binary hydride. In this case the H bonding states lie close to the Fermi level, as in binary titanium hydrides. It is known that the cubic phase is unstable at the appropriate H-concentration in the bulk titanium hydrides, and that tetragonal distortion of the lattice occurs in this case. In addition to changes in the interlayer distance between surface and subsurface layers in the thin film, the displacement of atoms in the lateral plane is also possible. The study of the plane reconstruction of the lattice upon adsorption requires  $c(2 \times 2)$  surface ES calculations, which involve a large amount of computing time.

For the stable adsorption geometry with the H atoms located in the Fe- or Ti-bridge position, H–Fe and H–Ti bonding states appear below the bottom of the d-band for the clean TiFe (110) surface (Fig. 9), as in the case of H in the hollow position for B2 TiFe (001). These states are strongly localized in the top layer of the substrate and on the adsorbate atoms. The formation of bonding H–Me states at high binding energies is accompanied by a depletion of the d-states in the lower part of the d-band. In addition, we find a pronounced change in the shape of the d–Me band in the surface layer in comparison with the clean surface, which may be directly related to a preferred interaction of the H s-states with the Fe or Ti d-states of different symmetry, depending on the adsorption site. These interactions could be responsible for the local chemical reactivity of the TiFe (110) surface. It is obvious that the surface chemical reactivity in an ordered TM alloys is very local, since the LDOS on each site is different in the alloys. A more detailed investigation of H adsorption onto the TiFe (110) surface will be presented in a forthcoming paper. Calculation of the adsorption energy curve versus H distance above the surface requires a large amount of computing time. It is known that the adsorption curves obtained for CO on a NiAl (110) surface are very sensitive to the choice of exchange-correlation potential used in the calculation [13]. However, a small influence of non-local exchange-correlation corrections on the atomic hydrogen adsorption process and on the relaxation of the substrate was found only for the pure TM [10]. The change in the adsorption energy was obtained due to the binding energy of the hydrogen molecule corrected by GGA [32]. The influence of non-local exchange-correlation

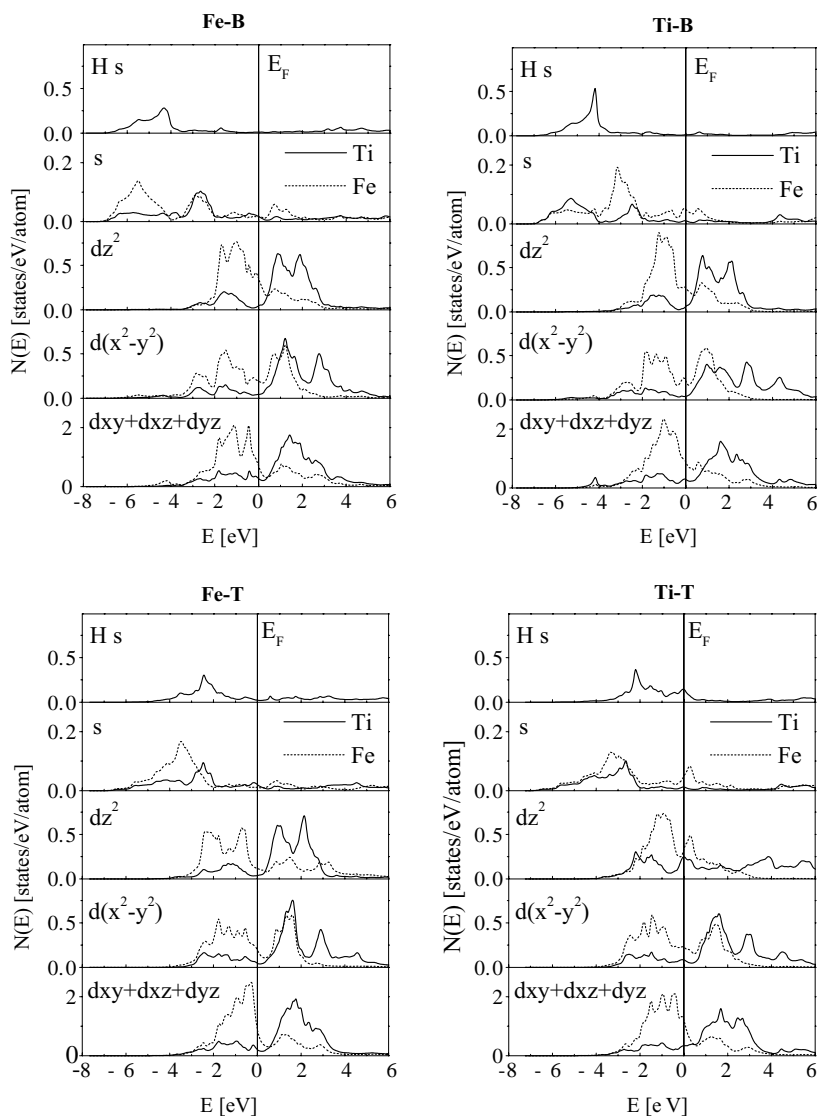


Fig. 8. Partial DOS in the surface layer of substrate in TiFe (110) films with H in Ti-B, Fe-B, Ti-T, Fe-T position, respectively.

correction on the hydrogen adsorption onto TM alloy surfaces needs to be investigated in greater detail.

#### 4. Conclusion

The present calculations predict ferromagnetic ordering on the Fe-terminated TiFe (001) surface with a magnetic moment of  $2.27\mu_B$  for the Fe atoms. This ordering rapidly diminishes inside film. Our results also reveal a small induced polarization of  $-0.41\mu_B$  for Ti-subsurface atoms. The adsorption of atomic H in the stable fourfold hollow position on the TiFe (001) surface was found to be very similar for the two surface terminations in non-magnetic calculations.

However, the magnetic ordering in the Fe-terminated (001) surface causes H adsorption on the Ti-terminated (001) surface to be preferable. The present results also show a small induced magnetic moment of  $0.23\mu_B$  for the surface Ti atoms upon hydrogenation, while hydrogen significantly influences the magnetic moment of the Fe atoms in both the surface and subsurface layers. Four different geometries for hydrogen adsorption onto the (110) surface were also investigated. The significant changes in ES observed in the hydrogen-containing surfaces are connected primarily with the formation of strongly hybridized H s-states with the Fe or Ti s- and d-bonding states. In addition, these interactions are strongly influenced by the position of the adsorbed hydrogen. During hydrogen charging the density of states at

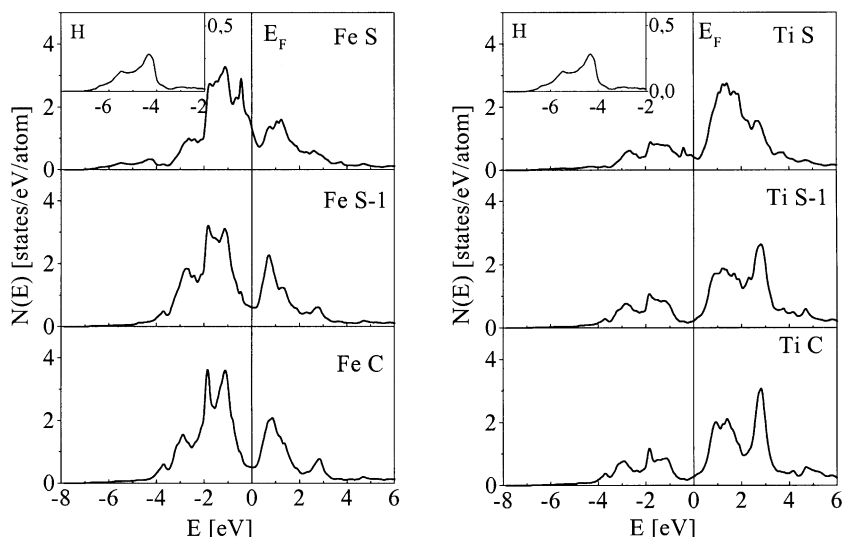


Fig. 9. LDOS in the layers of substrate and on the hydrogen Fe “bridge” site (in the inset) for H-covered TiFe (110).

the Fermi level increases in all the cases considered, which causes a weakening of interatomic bonds and phase instability.

### Acknowledgements

This work was partly supported by a collaborative program between the Institute of Strength Physics and Materials Science RAS, Tomsk, Russia and the Basic Science Research Institute, Pohang University of Science and Technology, Republic of Korea. It was jointly funded by the KOSEF-2001 research fund.

### References

- [1] Mankovsky SV, Tcherepin VT. *Metallofizika i noveyshie tehnologii* 1997;19:57–61.
- [2] Mankovsky SV, Ostroukhov AA, Floka VM, Tcherepin VT. *Vacuum* 1997;48:245–7.
- [3] Koroteev YuM, Lipnitskii AG, Chulkov EV, Naumov II. *Phys Low-Dim Struct* 1998;9/10:85–92.
- [4] Amalou F, Benakki M, Mokrani A, Demangeat C. *Eur Phys J B* 1999;9:149–57.
- [5] Canto G, de Coss R. *Surf Sci* 2000;465:59–64.
- [6] Lee G, Kim JS, Koo YM, Kulkova SE, Valujsky DV. *Phys Low-Dim Struct* 2001;5/6:19–36.
- [7] Kulkova SE, Valujsky DV, Lee G, Kim JS, Koo YM. *Physica B* 2001;304:186–92.
- [8] Fernando GW, Wilkins JW. *Phys Rev B* 1987;35:2995–8.
- [9] Huang H, Hermanson J. *Phys Rev B* 1985;32:6312–8.
- [10] Eichler A, Hafner J, Kresse G. *J Phys: Condens Matter* 1996;8:7659–75.
- [11] Hammer B, Scheffler M. *Phys Rev Lett* 1995;74:3487–90.
- [12] Bihlmayer G, Eibler R, Podloucky R. *Surf Sci* 1998; 402–404:794–7.
- [13] Bihlmayer G, Eibler R, Podloucky R. *Surf Sci* 2000;446: 188–92.
- [14] Lozovoi AY, Alavi A, Finnis M. *Phys Rev Lett* 2000;85: 610–6.
- [15] Ostanin S, Uzdin VM, Demangeat C, Wills JM, Alouani M, Dreyse H. *Phys Rev B* 2000;61:4870–6.
- [16] Jain IP, Devi B, Sharma P, Williamson A, Vijay YK, Avasthi DK, Tripathi A. *Int J Hydrogen Energy* 2000;25:517–21.
- [17] Papaconstantopoulos DA, Nagel DJ. *Int J Quant Chem* 1971;55:515–21.
- [18] Yamashita J, Asano S. *Prog Theor Phys* 1972;48:2119–23.
- [19] Gupta M. *J Phys F: Met Phys* 1982;12:L57–62.
- [20] Papaconstantopoulos DA, Switendick AC. *Phys Rev B* 1985;32:1289–94.
- [21] Kulkova SE, Valujsky DV, Smolin Iyu. *Izvestiya VUZov Fisika* 2000;9:56–63.
- [22] Thompson P, Pick M, Reidinger F, Corliss LM, Hastings J, Reilly J. *J Phys F: Met Phys* 1978;8:L75–80.
- [23] Reilly J, Wiswall R. *Inorg Chem* 1974;13:218–22.
- [24] Blaha P, Schwarz K, Luitz J. WIEN97. Vienna University of Technology, 1997. 161p. (Improved and updated Unix version of the origin copyrighted WIEN-code, which was published by Blaha P, Schwarz K, Sorantin P, Trickey SB. *Comput Phys Commun* 1990;59:399).
- [25] Lee G, Kim JS. Parallelization of the FLAPW method: MPI implementation. POSTECH internal Report, 1999. 16p.
- [26] Brandes EA, Brook GB. *Smithells Metals Reference Book*, 7th ed. London: Butterworth-Heinemann, 1992.
- [27] Yu R, Singh D, Krakauer H. *Phys Rev B* 1991;43:6411.
- [28] Talanana M, Benakki M, Amalou F, Bouarab S, Demangeat C. *Eur Phys J B* 2001;22:497–503.
- [29] Lee J, Fu C, Freeman A. *Phys Rev B* 1987;36:9318–23.
- [30] Lui S, Davenport J, Plummer E, Zehner D, Fernando G. *Phys Rev B* 1990;42:13250–4.

- [31] Bihlmayer G, Asada T, Blugel S. *Phys Rev B* 2000;62:11937–40.
- [32] Perdew JP, Burke S, Ernzerhof M. *Phys Rev Lett* 1996;77:3865–70.
- [33] Spisak D, Hafner J. *Phys Rev B* 2000;61:4160–4.
- [34] Hammer B, Norskov JK. *Surf Sci* 1995;343:211–8.
- [35] Huber KP, Herzberg G. *Constants of diatomic molecules. In molecular structure and molecular spectra IV*. New York: Van Nostrand-Reinhold, 1979.
- [36] Varma CM, Wilson AJ. *Phys Rev B* 1980;22:3795–804.
- [37] Yukawa H, Takahashi Y, Morinaga M. *Comp Mat Sci* 1999;14:291–4.